Journal of Engineering and Applied Technology
Vol. 5, No. 1, March 2024, pp. 01-10

Online ISSN 2716-2265
Printed ISSN 2716-2257

Stereolithography 3D printing for the investigation of acoustic focusing

Burhan Febrinawarta[1,*], Adhika Widyaparaga[1], I Made Miasa[1], Sucipto[1], Witnadi Dardjat Premiaji[1]

[1]Department of Mechanical and Industrial Engineering, Universitas Gadjah Mada, Indonesia
E-mail: burhanfebrinawarta@ugm.ac.id *
* Corresponding Author

ABSTRACT

In our environment, acoustic sound waves transform into undesirable noise when their intensity exceeds 100 dB, prompting a need for effective mitigation strategies. In recent years, there has been increasing interest in utilising sound/noise and acoustics for energy harvesting, especially for low-power electronic devices committed to clean renewable energy sources. Metamaterials, with a spotlight on metalens, are emerging as a promising solution for precise sound focusing and energy conservation. This study delves into the intricate process of fabricating metalens through Stereolithography (SLA) 3D printing, unravelling their acoustic focusing capabilities. Metalenses, equipped with intricately designed labyrinthine unit cells tailored for manipulating reflected wave phases, materialize through the precision of SLA 3D printing, forming a sophisticated multilateral structure. The experimental framework for acoustic focusing integrates essential components such as a waveguide, speaker array, metalens, acoustic foam, and a sound level meter. The resultant metalens, composed of 22-unit cells with diverse dimensions, distinctly demonstrate robust acoustic focusing capabilities. Calibration procedures are systematically applied to ensure uniformity of speaker array output and to create a carefully controlled acoustic environment. Sound level measurements clearly depict zones of mutually reinforcing resonance heights, while, conversely, there are also zones of mutually attenuating sound. The complex interplay of sound waves through the metalens, intricately guided by the design of the unit cells, decisively determines the degree of acoustic focus achieved. The SLA 3D printed metalens emerges as a compelling manifestation of effective sound concentration, poised for potential applications in the realm of acoustic energy harvesting. Nevertheless, the study's consequential findings beckon further scientific exploration, prompting an in-depth comprehension of the nuanced impacts of input frequency and potential heating phenomena.

ARTICLE INFO

Article history
Received:
2 March 2024
Revised:
27 March 2024
Accepted:
31 March 2024

Keywords
acoustic focusing
acoustic lens
metalens
stereolithography

1. Introduction

Acoustic sound waves, which are mechanical waves containing energy, can be produced by numerous noise sources. When these sound waves are unwanted, they are termed as noise. Common sources of noise comprise aeroplanes [1], high-speed trains [2], vehicles [3], power plants [4], machinery [5], and loudspeakers [6]. In the present era, humans inhabit a world characterized by heightened noise levels, where acoustic energy serves as an essential component of the environment. In our environment, sound levels frequently surpass 100 dB, and the prevalence of low-frequency noise tends to control the frequency spectrum [1], [2], [4].

In recent years, the study of sound and acoustics has become increasingly important in the field of energy harvesting [7]. The development of low-power electronic devices has led to the exploration of clean, renewable energy sources, and sound has emerged as a promising option. Despite its abundance

in various environments, the energy density of sound is relatively low compared to other ambient energy sources. Hence, it is necessary to focus or confine sound energy through effective conversion media for better Acoustic Energy Harvesting (AEH) [6].

One of the key challenges in AEH is the low frequency and low amplitude of the ambient sound. To overcome this challenge, researchers have explored various methods to enhance the sound energy density, such as resonant structures, microperforated panels, and metamaterials. Among these methods, metamaterials have shown great potential for sound focusing and energy confinement due to their unique properties, such as negative refraction and subwavelength resonances [8]–[11].

Metamaterials are artificially engineered materials that possess properties not found in natural materials. These materials consist of subwavelength resonators capable of controlling the phase and amplitude of incoming sound waves. This capacity facilitates the creation of customized acoustic properties, such as negative refraction, superlensing, and cloaking. These unique properties have made metamaterials a promising platform for sound focusing and energy confinement [8]–[12].

Metalenses, employed to concentrate sound, belong to the category of metamaterials utilized for the focalization of either light or sound. These metalenses are characterized by their flat and thin structure. Their design is based on the theoretical phase-shift profile necessary for focusing reflected waves, a realization achieved by appropriately arranging labyrinthine units in specific sequences [9], [10], [13], [14]. The analysis and discussion delve into coupling effects and multiple reflections occurring among or between metalenses. The findings illustrate that acoustic focusing and confinement exhibit enhancement with the increasing sides of the multilateral metalens [9], [10], [13], [14].

The metalens can be produced through additive manufacturing, commonly known as 3D printing, a process that fabricates three-dimensional solid objects from a digital file. This method enables the creation of intricate 3D structures with minimal weight and zero material wastage, distinguishing it from traditional manufacturing practices. Additive manufacturing encompasses a broad spectrum, ranging from printing parts in plastics to metals [13]. Various additive manufacturing technologies, such as Stereolithography (SLA) and Fused Deposition Modelling (FDM) [14], are prevalent for producing items like jigs, fixtures, and tools. FDM is typically employed for crafting straightforward components, whereas SLA excels in developing intricate and highly precise components [15]. Given the metalens's demand for precision and a smooth surface, the preferred 3D printing method is SLA. Stereolithography, known for its high precision, is a 3D printing method that constructs three-dimensional objects by layering thin sheets of UV-curable polymers, such as acrylic resin and rubber, and then curing them using UV light radiation [16]–[18].

Noise remains an integral part of our world, and if harnessed effectively, it could yield significant advantages. One such application involves focusing noise, which opens up the possibility of deriving benefits from it, such as enhancing speaker output for optimal human listening comfort. However, achieving sound focus requires a validated method to ensure its efficacy. In this research, a fabrication of metalens using SLA 3D printing is conducted to investigate acoustic focusing. Furthermore, this study also undertakes a fundamental study on sound focusing to increase the intensity of the sound through experimentation. The proposed multilateral metasurfaces (metalens) have excellent performance in acoustic energy confinement and strong acoustic focusing capabilities, making them a promising platform for AEH. The results of this study have important implications for the development of sustainable energy sources.

2. Method

Metalens made up of a variety of unit cells, such as Helmholtz resonators and labyrinthine chambers, have demonstrated extraordinary wave-front shaping capabilities [7], [8]. In this paper, different labyrinthine unit cells are utilized as candidates to manipulate the phase of reflected waves by coiling

up space (space-coiled structure). The shifted phase of the reflected waves controlled by each unit is crucial to achieve the desired reflected field. As theoretically and experimentally validated in [8], [9], the thickness of the upper or lower plates, w, and the number of bars are the two essential configurable parameters to achieve the full 2π-range phase shift and maintain planar properties as well [8], [9].

In this research, we made a metalens using SLA 3D printing, and its details can be seen in Fig. 1. The process has a few main steps (see Fig. 2). First, in the design phase, the metalens was carefully designed using computer-aided design (CAD) software and then converted into STL format. This design process is crucial as considerations are made regarding both the lens's focusing capabilities and the material properties of the photopolymer utilized in SLA printing. Subsequently, the 3D design was sliced into thin layers using specialized slicing software. These sliced layers were then printed layer by layer using an SLA 3D printer, with the material being exposed to focused UV light to solidify each layer. Upon completion of the printing process, the metalens was removed from the printing platform and cleaned with a solvent to eliminate any excess material. Additional steps such as etching or polishing may have been performed to enhance its performance. Finally, the metalens was tested to assess its sound focusing capabilities.

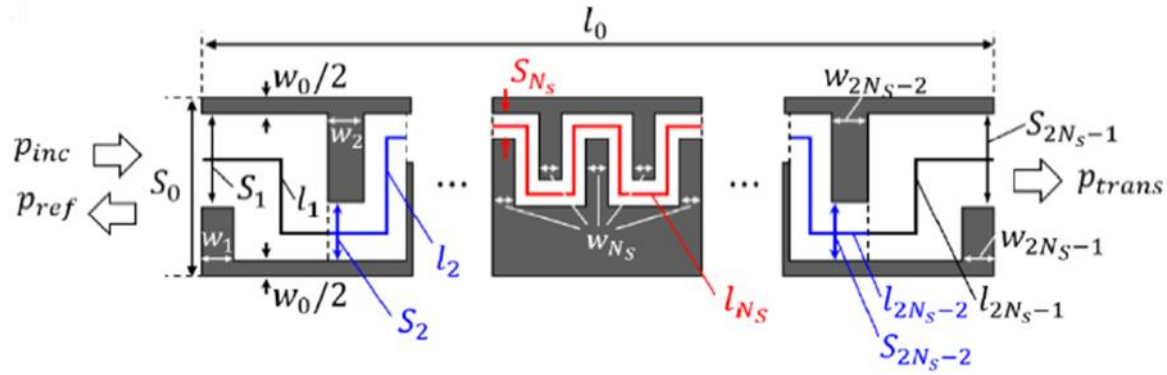

Fig. 1 The nomenclature of two-dimensional space-coiled structure (metalens) [8]

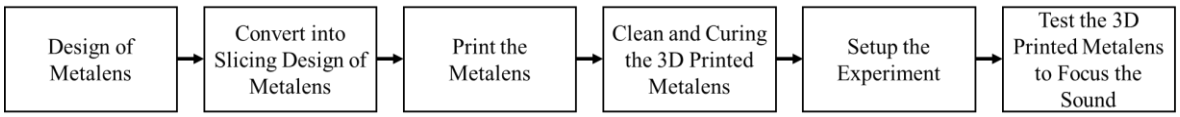

Fig. 2 The nomenclature of two-dimensional space-coiled structure (metalens) [8]

The geometry of the unit cell for a metalens is presented in Fig. 3. The dimensions and quantity of labyrinths within these unit cells play a crucial role in achieving effective sound focusing. The constructed metalens comprises 22-unit cells, each featuring 11 distinct types of unit cells arranged in a mirrored fashion. Despite variations in dimensions among the 11-unit cells, some dimensions, such as S0 at 22 mm, w0 at 1 mm, and L0 at 108.6 mm, remain consistent. The arrangement of the unit cells within the metalens is illustrated in Fig. 4. The unit cells of the metalens were produced using the Anycubic Photon Mono X SLA 3D printer, employing Anycubic 405 nm Resin. To translate the pattern design (in STL format) into G codes, the Photon Workshop software served as the slicing tool. The selection of SLA printing over FDM was based on its capability to deliver higher precision and smoother

surfaces in the printed components. For the unit cell printing, a slicing layer thickness parameter of 50 microns was opted for to ensure accurate and precise printing results.

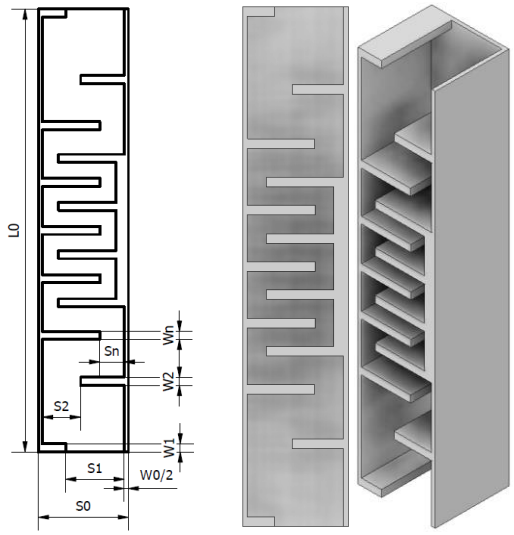

(a) (b)

Fig. 3 The geometry of a unit cell for a metalens: (a) parameter of unit cell and (b) 3D model

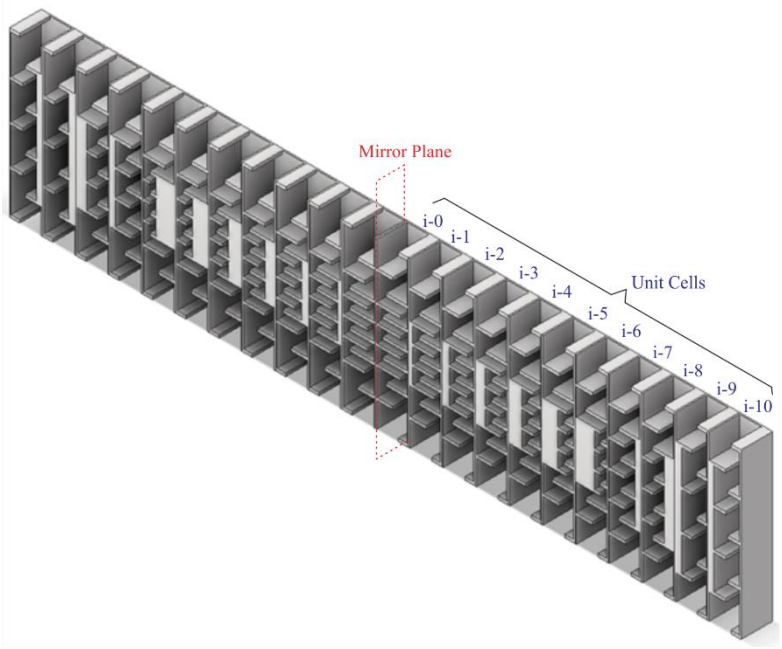

Fig. 4 The design of unit cell arrangement on metalens

The experimental arrangement, detailed in Fig. 5, encompasses a comprehensive setup. It includes a waveguide formed by two glass plates (1000 x 500 x 3 mm), a speaker array (8 small speakers 5W 40 x 70 mm), a metalens, acoustic foam, and a sound level meter. Prior to initiating the experiment, meticulous calibration procedures were implemented. This calibration involved ensuring the sound level meter was precisely calibrated. Additionally, a calibration process for the speaker output was conducted

to guarantee uniformity, ensuring that the output of each speaker falls within a specified range, as depicted in Fig. 6.

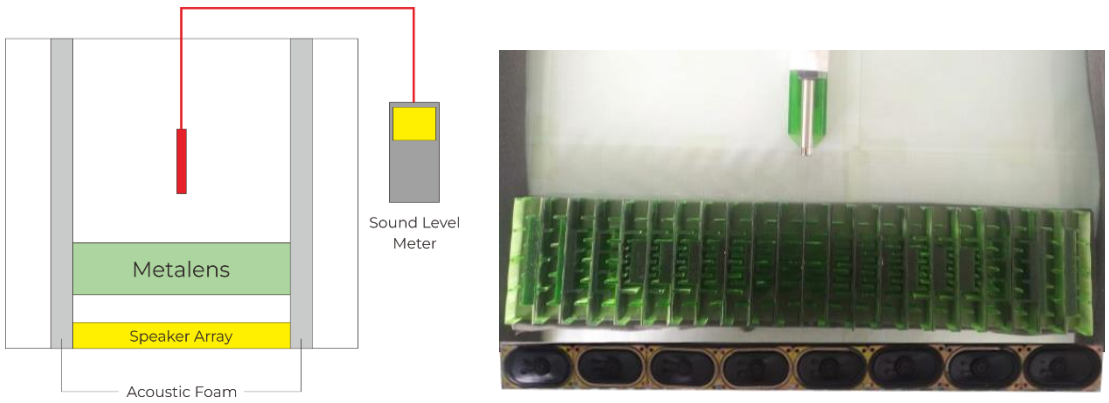

(a) (b)

Fig. 5 (a) The schematic of experiment setup and (b) experiment setup (exploded view)

Fig. 6 Speaker output calibration

The procedural methodology for this experiment involves a systematic approach: (a) initialization by setting up the experimental apparatus; (b) the initiation of the speaker emitting sound at a predefined frequency, specifically set at 1000 Hz for the current study; and (c) the precise measurement of sound levels at designated points, employing a sophisticated sound level meter. The instrument of choice for this purpose is the LT Lutron SL-4013, notable for its extensive reading range spanning from 31.5 to 8000 Hz and a dynamic range of 30 to 130 dB.

3. Results and Discussion

The conceptualization of unit cell configurations has undergone meticulous design (see Fig. 3 and Fig. 4), and subsequent to this phase, the unit cells have been actualized through the implementation of an SLA 3D printer, as illustrated in Fig. 7. Furthermore, the arrangement of these unit cells has been executed in a manner that results in the cohesive formation of a metalens, as visually depicted in Fig. 8.

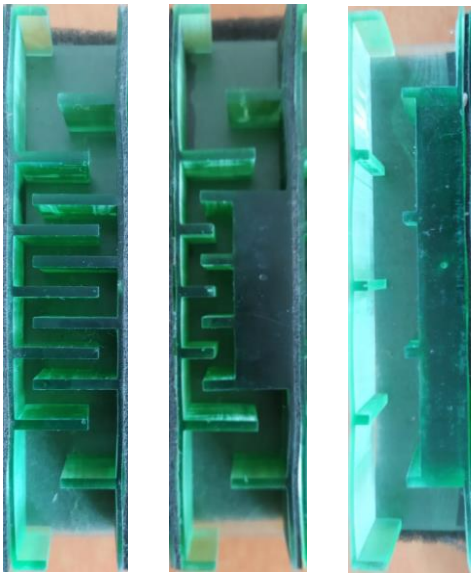

(a) (b) (c)

Fig. 7 The printed unit cell: (a) i-0; (b) i-5; and (c) i-10

Fig. 8 The printed metalens

The speaker output calibration process was methodically conducted, aiming for precision and consistency in the acoustic setup. This calibration was designed to ascertain that each speaker uniformly produced sound within a predefined range. The outcome of this calibration effort revealed an average output value for the entire speaker array, registering at 89.8 $\pm$ 2.4 dB. Further scrutiny indicated a tightly clustered range, with individual speaker outputs fluctuating within the interval of 88.2 dB to 90.6 dB. This meticulous calibration lays a robust foundation for the subsequent acoustic experimentation, ensuring a controlled and standardized auditory environment.

The coordinate system employed for measurement is delineated in Fig. 9 (a). The measurement outcomes along the X-axis and Y-axis are elucidated in Fig. 9 (b) and (c), respectively. As depicted in Fig. 9 (b), the peak of intensity is observed at X = 0 mm, denoting a focal point of sound energy concentration. Correspondingly, Fig. 9 (c) unveils the zenith of intensity at Y = 100 mm. These apices signify regions where sound waves passing through the metalens synergistically reinforce one another. Conversely, the nadir of intensity is evident at X = -150 mm, X = 150 mm, and Y = 200 mm, indicative of regions where sound waves negate each other, resulting in attenuated acoustic signals.

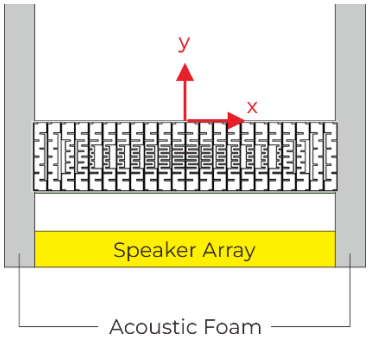

(a)

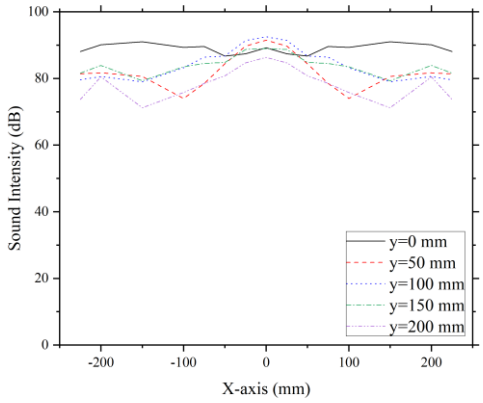

(b)

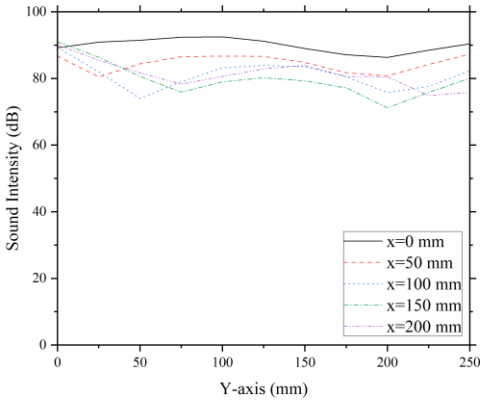

(c)

Fig. 9 (a) The coordinate of X and Y; (b) The results of measurement along X-axis; and (c) The results of measurement along Y-axis

As evident from the observations depicted in Fig. 10, there is a distinct concentration of sound at specific coordinates, precisely X = 0 and Y = 100, when the frequency is set at 1000 Hz. Additionally, zones experiencing sound cancellation are observed at coordinates (-225, 225) and (225,225). Upon traversing the metalens, an intriguing acoustic phenomenon unfolds, revealing a nuanced interplay of focused sound zones and the cancellation of sound waves. This intricate behaviour can be attributed to the varied phases of individual waves navigating the unit cell structure within the metalens. The ensuing interference patterns among the emitted sounds are contingent upon the relative phase differences inherent in each wave.

An intriguing insight emerges when sounds passing through the metalens exhibit congruent phase differences, they cohesively amplify, culminating in the creation of intensified acoustic zones. Conversely, disparate phase differences lead to the cancellation of these sound zones. Consequently, the effectiveness of sound focusing is intricately tied to the intricate design of the unit cell and the specific frequency of the acoustic output. This underscores the critical influence wielded by these parameters in determining the precise degree of acoustic focus achieved. Building upon the findings of previous research [8], it was revealed that by employing an alternative metalens design and adjusting the input frequency to 4 kHz, notable variations in sound intensity values were observed. Specifically, the results indicated that at distinct spatial coordinates, namely X=0 mm and Y=250 mm, sound intensity values

reached significant levels. This divergence in outcomes underscores the sensitivity of sound focusing phenomena to the intricacies of metalens design and input parameters.

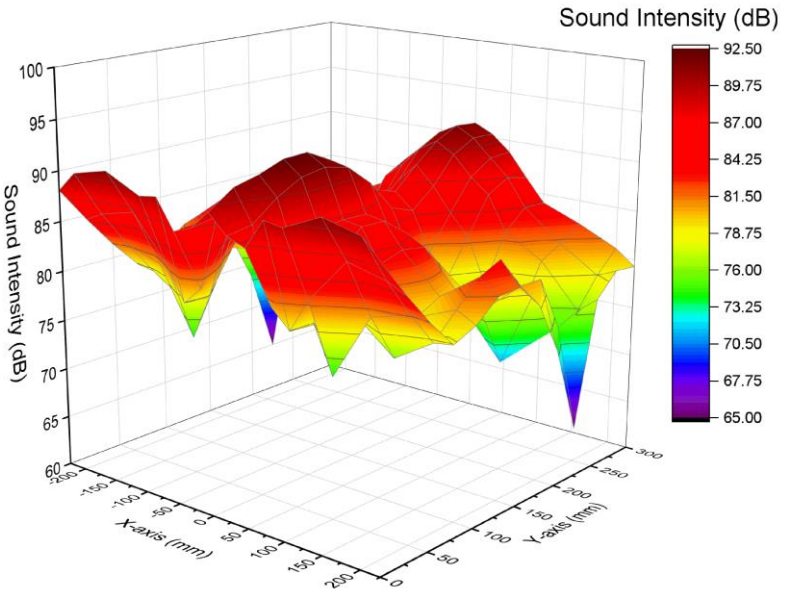

(a)

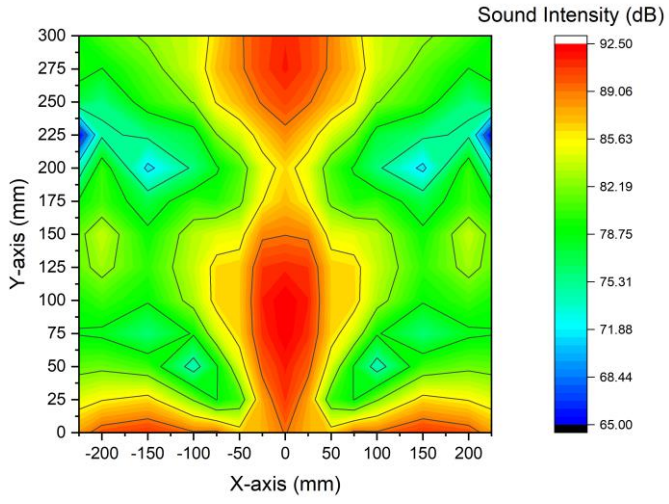

(b)

Fig. 10 Mapping of the results from measurements using a sound level meter (frequency of 1000 Hz); (a) 3D map and (b) contour map

Hence, it can be deduced that, at a frequency of 1000 Hz, the configuration of these metalenses, comprising 11 pairs of symmetrical unit cells, facilitates the generation of a focal point for sound intensity at X = 0 mm and Y = 100 mm. Furthermore, the localization of the sound intensity's focal point subsequent to traversal through the metalens is contingent upon various parameters inherent in the experimental setup, including the metalens design and the input frequency of the speaker array.

4. Conclusion

In this study, the SLA 3D printing method was employed for the fabrication of metalens, with the aim of scrutinizing their capacity to concentrate sound. Subsequently, a systematic series of experiments was conducted to gain a more profound understanding of the acoustic focusing process. The efficacy of sound concentration by metalens was unequivocally demonstrated by the findings. Throughout the experimental procedures, a meticulous examination of sound patterns subsequent to their interaction with the metalens was conducted. Clear distinctions were observed, delineating zones characterized by heightened sound intensity, reaching peaks of 92.5 dB (at coordinates 0, 100), contrasted with areas exhibiting diminished sound intensity, registering at 65 dB (at coordinates -225, 225, and 225, 225), all at a frequency of 1000 Hz and with a specific configuration of 11 pairs of metalens. Importantly, the precision of sound focus was found to be contingent upon the intricate design intricacies of the unit cell within the metalens.

Recommendation

Despite these significant findings, acoustic focusing is influenced by numerous factors, warranting further exploration. For instance, the influence of input frequency on acoustic focusing and the investigation of potential heating phenomena are considered potential areas for future research. The considerable potential inherent in the application of sound-focusing materials such as metalens across various scenarios is underscored by these discoveries. This concept introduces a novel and potentially transformative solution to enhance efficiency and sound quality in diverse applications. Beyond the confines of the laboratory, this breakthrough has the potential to revolutionize the improvement of sound-related technologies in practical real-world applications.

Acknowledgement

This work was financially supported by “Hibah Penelitian Departemen Teknik Mesin dan Industri Fakultas Teknik, Universitas Gadjah Mada” (1501407/UN1.FTK/SK/HK/2022) and Dynamics Laboratory, Department of Mechanical and Industrial Engineering, Faculty of Engineering, Gadjah Mada University.

References

[1] J. Ivošević, T. Bucak, and P. Andraši, “Effects of interior aircraft noise on pilot performance,” *Appl. Acoust.*, vol. 139, no. March, pp. 8–13, 2018, doi: 10.1016/j.apacoust.2018.04.006.

[2] H. M. Noh, “Acoustic energy harvesting using piezoelectric generator for railway environmental noise,” *Adv. Mech. Eng.*, vol. 10, no. 7, pp. 1–9, 2018, doi: 10.1177/1687814018785058.

[3] A. Pascale *et al.*, “Road traffic noise monitoring in a Smart City: Sensor and Model-Based approach,” *Transp. Res. Part D Transp. Environ.*, vol. 125, no. June, p. 103979, 2023, doi: 10.1016/j.trd.2023.103979.

[4] M. R. Monazzam *et al.*, “Investigation of occupational noise annoyance in a wind turbine power plant,” *J. Low Freq. Noise Vib. Act. Control*, vol. 38, no. 2, pp. 798–807, 2019, doi: 10.1177/1461348418769162.

[5] W. Yu-qin and D. Ze-wen, “Influence of blade number on flow-induced noise of centrifugal

pump based on CFD/CA," *Vacuum*, vol. 172, no. August 2019, p. 109058, 2020, doi: 10.1016/j.vacuum.2019.109058.

[6] M. Yuan, Z. Cao, J. Luo, and X. Chou, "Recent developments of acoustic energy harvesting: A review," *Micromachines*, vol. 10, no. 1, 2019, doi: 10.3390/mi10010048.

[7] Y. Wang *et al.*, "A renewable low-frequency acoustic energy harvesting noise barrier for high-speed railways using a Helmholtz resonator and a PVDF film," *Appl. Energy*, vol. 230, no. July, pp. 52–61, 2018, doi: 10.1016/j.apenergy.2018.08.080.

[8] C. Kim, J. Kim, and W. Jeon, "Realization of an acoustic metalens exhibiting broadband high transmission," *J. Sound Vib.*, vol. 529, Jul. 2022, doi: 10.1016/j.jsv.2022.116910.

[9] S. Qi, Y. Li, and B. Assouar, "Acoustic Focusing and Energy Confinement Based on Multilateral Metasurfaces," *Phys. Rev. Appl.*, vol. 7, no. 5, May 2017, doi: 10.1103/PhysRevApplied.7.054006.

[10] A. Spadoni and C. Daraio, "Generation and control of sound bullets with a nonlinear acoustic lens," *Proc. Natl. Acad. Sci. U. S. A.*, vol. 107, no. 16, pp. 7230–7234, Apr. 2010, doi: 10.1073/pnas.1001514107.

[11] C. M. Donahue, P. W. J. Anzel, L. Bonanomi, T. A. Keller, and C. Daraio, "Experimental realization of a nonlinear acoustic lens with a tunable focus," *Appl. Phys. Lett.*, vol. 104, no. 1, Jan. 2014, doi: 10.1063/1.4857635.

[12] G. do Gildean, E. F. Vergara, L. R. Barbosa, A. Lenzi, and R. S. Birch, "Sound absorption metasurface with symmetrical coiled spaces and micro slit of variable depth," *Appl. Acoust.*, vol. 183, p. 108312, 2021, doi: 10.1016/j.apacoust.2021.108312.

[13] D. S. Nagaraju, R. L. Krupakaran, C. Sripadh, G. Nitin, and G. Joy Joseph Emmanuel, "Mechanical properties of 3D printed specimen using FDM (Fused deposition modelling) and SLA (Stereolithography) technologies," *Mater. Today Proc.*, no. September, 2023, doi: 10.1016/j.matpr.2023.09.223.

[14] S. Wickramasinghe, T. Do, and P. Tran, "FDM-Based 3D printing of polymer and associated composite: A review on mechanical properties, defects and treatments," *Polymers (Basel).*, vol. 12, no. 7, pp. 1–42, 2020, doi: 10.3390/polym12071529.

[15] V. D. Sagias, K. I. Giannakopoulos, and C. Stergiou, "Mechanical properties of 3D printed polymer specimens," *Procedia Struct. Integr.*, vol. 10, pp. 85–90, 2018, doi: 10.1016/j.prostr.2018.09.013.

[16] C. Curti, D. J. Kirby, and C. A. Russell, "Systematic screening of photopolymer resins for stereolithography (SLA) 3D printing of solid oral dosage forms: Investigation of formulation factors on printability outcomes," *Int. J. Pharm.*, vol. 653, no. January, p. 123862, 2024, doi: 10.1016/j.ijpharm.2024.123862.

[17] M. Kurimoto, Y. Manabe, S. Mitsumoto, and Y. Suzuoki, "Layer interface effects on dielectric breakdown strength of 3D printed rubber insulator using stereolithography," *Addit. Manuf.*, vol. 46, no. March, p. 102069, 2021, doi: 10.1016/j.addma.2021.102069.

[18] H. Bin Lee, M. J. Noh, E. J. Bae, W. S. Lee, and J. H. Kim, "Accuracy of zirconia crown manufactured using stereolithography and digital light processing," *J. Dent.*, vol. 141, no. January, p. 104834, 2024, doi: 10.1016/j.jdent.2024.104834.